Biogeosciences, 11, 833–842, 2014
www.biogeosciences.net/11/833/2014/
doi:10.5194/bg-11-833-2014

Biogeosciences Open Access

Polar coralline algal $CaCO_3$-production rates correspond to intensity and duration of the solar radiation

S. Teichert[1] **and A. Freiwald**[2]

[1]GeoZentrum Nordbayern, Section Palaeontology, Erlangen, Germany
[2]Senckenberg am Meer, Section Marine Geology, Wilhelmshaven, Germany

Correspondence to: S. Teichert (sebastian.teichert@fau.de)

Received: 5 July 2013 – Published in Biogeosciences Discuss.: 26 August 2013
Revised: 8 January 2014 – Accepted: 8 January 2014 – Published: 11 February 2014

Abstract. In this study we present a comparative quantification of $CaCO_3$ production rates by rhodolith-forming coralline red algal communities situated in high polar latitudes and assess which environmental parameters control these production rates. The present rhodoliths act as ecosystem engineers, and their carbonate skeletons provide an important ecological niche to a variety of benthic organisms. The settings are distributed along the coasts of the Svalbard archipelago, being Floskjeret (78°18′ N) in Isfjorden, Krossfjorden (79°08′ N) at the eastern coast of Haakon VII Land, Mosselbukta (79°53′ N) at the eastern coast of Mosselhalvøya, and Nordkappbukta (80°31′ N) at the northern coast of Nordaustlandet. All sites feature Arctic climate and strong seasonality.

The algal $CaCO_3$ production rates were calculated from fuchsine-stained, presumably annual growth increments exhibited by the rhodoliths and range from 100.9 g $(CaCO_3)\,m^{-2}\,yr^{-1}$ at Nordkappbukta to 200.3 g $(CaCO_3)\,m^{-2}\,yr^{-1}$ at Floskjeret. The rates correlate to various environmental parameters with geographical latitude being the most significant (negative correlation, $R^2 = 0.95$, $p = 0.0070$), followed by the duration of the polar night (negative correlation, $R^2 = 0.93$, $p = 0.0220$), the duration of the sea ice cover (negative correlation, $R^2 = 0.87$, $p = 0.0657$), and the annual mean temperature (positive correlation, $R^2 = 0.48$, $p = 0.0301$).

This points out sufficient light incidence to be the main control of the growth of the examined coralline red algal rhodolith communities, while temperature is less important. Thus, the ongoing global change with its rising temperatures will most likely result in impaired conditions for the algae, because the concomitant increased global runoff will decrease water transparency and hence light incidence at the four offshore sites. Regarding the aforementioned role of the rhodoliths as ecosystem engineers, the impact on the associated organisms will presumably also be negative.

1 Introduction

Coralline red algae are the most consistently and heavily calcified group of the red algae, and as such have been elevated to ordinal status (Corallinales Silva and Johansen, 1986). Their calcification process involves high magnesium calcite precipitation within the cell walls (Kamenos et al., 2009). They can also form rhodoliths, free-living structures composed mostly (> 50 vol.-%) of non-geniculate coralline red algae (Bosence, 1983), and those are widely distributed in marine habitats (Foster, 2001), having an excellent fossil record since at least the Hauterivian (Arias et al., 1995), probably earlier (e.g. Schlagintweit, 2004; Bucur et al., 2009). Rhodoliths and coralline red algae are known as important $CaCO_3$ producers from tropical (Chisholm, 2000) over temperate (Martin et al., 2006) to subpolar environments (Freiwald and Henrich, 1994) and can also act as ecosystem engineers sensu Jones et al. (1994): they form microhabitats by their own skeletal growth.

This skeletal growth directly depends on the $CaCO_3$ production rates of the algae, a factor whose significant controls still remain unclear. A variety of methods have been applied to calculate coralline red algal growth rates and $CaCO_3$ production rates, such as in situ growth experiments on living thalli (Adey and McKibbin, 1970; Payri, 1997; Steller et al., 2007), counting of presumed annual growth increments in

relation to weight (Bosence, 1980; Freiwald and Henrich, 1994), using Mg / Ca ratios relative to growth increments (Halfar et al., 2000; Schäfer et al., 2011), alizarin-staining (Bosence and Wilson, 2003; Foster et al., 2007) or calcofluor-white-staining (Maytone, 2010), and high-resolution analysis of ^{14}C values to identify pre- and post-bomb spike periods of skeletal growth (Frantz et al., 2000). Additionally, growth rates without quantification of spatial $CaCO_3$ production rates have been calculated for instance for subarctic (Halfar et al., 2011) and temperate (Kamenos et al., 2008) coralline red algae in order to use the algae as high-resolution climate recorders. These completely different approaches and the handling of miscellaneous coralline red algal species from different water depths and biogeographical zones (Table 1) make it nearly impossible to compare the results. In this study, the $CaCO_3$ production rates of four coralline red algal communities, consisting mainly of *Lithothamnion glaciale* Kjellman, 1883, are based on the counting of fuchsine-stained, presumably annual growth increments in relation to weight and density of the calcifying structures, the so-called protuberances. This approach, standardized for all sites, makes it possible to compare the particular $CaCO_3$ production rates in order to test the controlling factors for their significance. Once identified, these factors can be considered in the mirror of the ongoing global change, so the future impact on the coralline red algae and the associated organisms can be estimated.

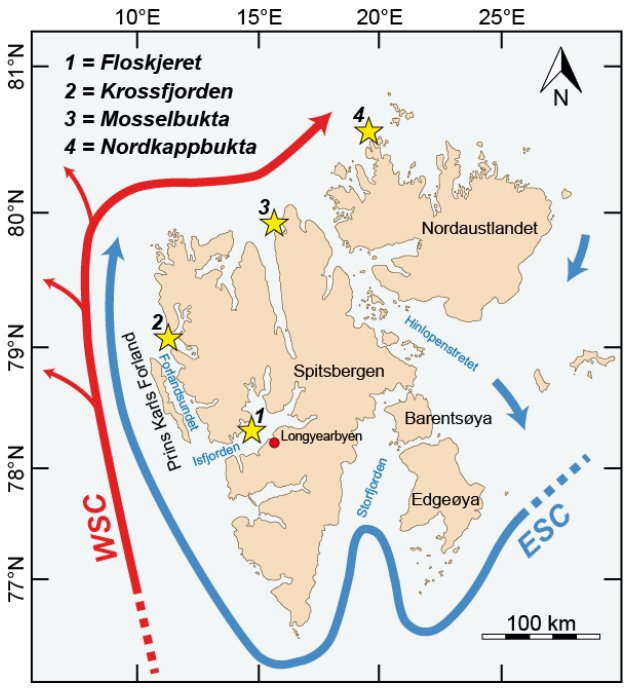

Fig. 1. The Svalbard archipelago with the four investigation sites (yellow stars); the water masses most influential on the local climate are the warm West Spitsbergen Current (WSC, red) and the cold East Spitsbergen Current (ESC, blue).

2 Materials and methods

2.1 Rhodolith and coralline red algal sampling

Samples and data were obtained from 31 July to 17 August in 2006 during the MSM 02/03 expedition of RV Maria S. Merian (Lherminier et al., 2009), heading around the Svalbard archipelago in an interdisciplinary approach and including the investigation of four sites dominated by coralline red algae and rhodoliths (Fig. 1). All sites are characterized by similar physical and biological environmental conditions, and the actual thriving of the coralline red algae is obvious. For a thorough description of the investigations at the coralline red algal and rhodolith beds and the associated environment, please refer to Teichert et al. (2012) for Nordkappbukta and to Teichert et al. (2014) for Floskjeret, Krossfjorden, and Mosselbukta. Rhodoliths and coralline red algae were collected using the following approach.

The seabed at each site was mapped using a Kongsberg EM 1002 multibeam echo sounder controlled with the software package SIS. The multibeam raw data were processed using the software packages Neptune and Cfloor, including the production of digital terrain models. These models were used to create suitable dive tracks for the manned submersible JAGO, which carried out the visual inspection and video documentation of the seafloor and the sampling of the rhodolith and coralline red algal communities with a hydraulic manipulator arm. Additionally, a dredge with an opening of 100 cm width and 40 cm height and a net of 0.5 cm mesh size was used for sampling. Samples were collected from one site at Floskjeret (757; Fig. 2a), three sites at Krossfjorden (637, 644, 652; Fig. 2b), one site at Mosselbukta (684; Fig. 2c), and three sites at Nordkappbukta (701, 711, 714; Fig. 2d). One sample from Nordkappbukta (714) was collected in significantly shallower waters in order to check the influence of water depth on the $CaCO_3$ production rates.

2.2 Sample preparation and calculation of $CaCO_3$ production rates

Coralline algal genera and species were determined using thin sections, histological slices, and samples for the scanning electron microscope (SEM, Tescan Vega\\XMU). Identification of thalli of *Lithothamnion glaciale* Kjellman, 1883, was based on Adey (1964, 1966, 1970), Adey et al. (2005), Irvine and Chamberlain (1994), and Kjellman (1883, 1885, containing the original account of *L. glaciale*). Collected rhodoliths were sorted, and only monospecific rhodoliths composed of *Lithothamnion glaciale* (Fig. 3a) were included to the calculation of the $CaCO_3$ production rates (Floskjeret, $n = 17$; Krossfjorden, $n = 48$; Mosselbukta, $n = 27$; Nordkappbukta, $n = 75$ (containing a control group from

Table 1. Compiled annual $CaCO_3$ production rates of coralline red algae per square metre per year from south to north. Additional information on the production rates of partly undetermined coralline red algal species is available in Basso (2012).

Locality	Lat. [°]	Depth [m]	species	$CaCO_3$ production [g ($CaCO_3$) m^{-2} yr^{-1}]	Reference
Arvoredo Island, Brazil	27.25° S	7–20	*Lithophyllum* sp.	55.0–136.3	Gherardi (2004)
Shark Bay, Australia	25.50° S	?	*Fosliella* sp., *Pneophyllum* sp.	30–300	Walker and Woelkerling (1988)
Lizard Island, Australia	14.67° S	0	*Hydrolithon onkodes*	10 300	Chisholm (2000)
Lizard Island, Australia	14.67° S	18	*Neogoniolithon conicum*	1500	Chisholm (2000)
Gulf of Chiriquí, Panama	07.60° N	12–53	*Lithothamnion* sp.	81.09	Schäfer et al. (2011)
Gulf of Panama, Panama	08.00° N	3–26	*Lithothamnion* sp.	23.38	Schäfer et al. (2011)
Barbados, Lesser Antilles	13.25° N	0–10	*Porolithon* sp.	2378	Stearn et al. (1977)
Barbados, Lesser Antilles	13.25° N	0–10	*Neogoniolithon* sp.	1225	Stearn et al. (1977)
Barbados, Lesser Antilles	13.25° N	0–10	*Lithophyllum* sp.	1355	Stearn et al. (1977)
Barbados, Lesser Antilles	13.25° N	0–10	*Mesophyllum* sp.	167	Stearn et al. (1977)
Penguin Bank, Hawaii	21.13° N	40–100	*Porolithon onkodes*	2100	Agegian et al. (1988)
Cilento Shelf, Italy	40.30° N	47	*Lithothamnion corallioides*	90.8	Savini et al. (2012)
Mallorca–Menorca, Spain	40.50° N	0–10	*Neogoniolithon brassica-florida*	289.4	Canals and Ballesteros (1997)
Marseilles, France	43.28° N	0.5–1	*Corallina elongata*	5037	El Haïkali et al. (2004)
Bay of Brest, France	48.33° N	1–10	*Lithothamnion corallioides*	150–3000	Martin et al. (2006)
Bay of Brest, France	48.35° N	0–10	*Lithothamnion corallioides*	876	Potin et al. (1990)
Manorbier, GB	51.64° N	< 1	*Lithophyllum incrustans*	378.96	Edyvean and Ford (1987)
West Angle Bay, GB	51.69° N	< 1	*Lithophyllum incrustans*	59.76	Edyvean and Ford (1987)
Mannin Bay, Ireland	53.46° N	< 10	*Lithothamnion corallioides*	29–164	Bosence (1980)
Mannin Bay, Ireland	53.46° N	< 10	*Phymatolithon calcareum*	79–249	Bosence (1980)
Mannin Bay, Ireland	53.46° N	< 10	*Lithothamnion corallioides*	212–1197	Bosence and Wilson (2003)
Straumen Bioherm, Norway	69.67° N	18–20	*Lithothamnion* cf. *glaciale*	420–630	Freiwald and Henrich (1994)
Storvoll Reef, Norway	70.00° N	7	*Lithothamnion* cf. *glaciale*	895–1432	Freiwald and Henrich (1994)

shallower waters, station 714, $n = 37$)). The upper living surfaces (i.e. the part where $CaCO_3$ production occurs) of the rhodoliths together with a 5 cm scale were photographed with a Zeiss 50 mm Macro mounted on a Nikon D200 DSLR and the software Nikon Capture Control. The software Olympus analySIS FIVE was used to calibrate the images with the 5 cm scale in order to measure the area of the living surface and to count the protuberances (i.e. the main spots of $CaCO_3$ production; Fig. 3b). The resulting median numbers of protuberances per area [n m^{-2}] were checked for coherence using Levene's test for homogeneity of variance based on means (one-way ANOVA).

Five protuberances each of randomly selected rhodoliths were cut off, longitudinal measured using a Hazet digital calliper, dried in a Memmert 700 cabinet desiccator at 40 °C for 48 h, and weighed using a Mettler Toledo AB204-S classic precision balance. Processed protuberances were embedded using Araldit BY 158 resin (100 parts) and Aradur 21 hardener (28 parts), longitudinal cut using a water-cooled low-speed diamond saw, and wet-polished with SiC powder (220, 400, and 800 graining). Polished sections were etched with 0.1 n HCl for 3 s and stained with fuchsine solution (1 g fuchsine in 100 mL ethanol 50 %) for 10 s to amplify the growth increments (Fig. 3c). Assuming an annual pattern, growth increments per protuberance were counted using a Zeiss Stemi 2000 stereo microscope. If growth increments could not be distinguished clearly, the annual forming conceptacles (i.e. the chambers containing spores; Fig. 3a, c) were used as a substitute. Increment numbers were plotted against the weight of the whole protuberance to check if growth succession was linear using reduced major axis algorithm and Levene's test for homogeneity of variance based on means (one-way ANOVA). Subsequent increment counting led to the mean amount of produced $CaCO_3$ per protuberance per year [g ($CaCO_3$) yr^{-1}], which was checked for significance using Levene's test for homogeneity of variance based on means (one-way ANOVA). Together with the calculated number of protuberances per square metre, the annual $CaCO_3$ production per square metre per year [g ($CaCO_3$) m^{-2} yr^{-1}] was calculated by multiplication of the values.

The resulting $CaCO_3$ production rates (excluding the shallow water control group from Nordkappbukta) were plotted against the physical parameters water depth, seawater calcite saturation (snapshot conditions recorded during MSM 02/03 expedition of RV Maria S. Merian; see also Teichert et al. (2012, 2014)), annual mean temperature (data from LEVITUS 94, 2013), duration of sea ice cover (data from Svendsen et al., 2002; Nilsen et al., 2008; Spreen et al., 2008; AMSR-E Sea Ice Maps, 2013), geographical latitude, and duration of the polar night (data from USNO Sun Rise Tables, 2013) at each site. The results were checked for correlations using reduced major axis algorithm and Levene's test for homogeneity of variance based on means (one-way ANOVA). Correlating factors were checked for their relative influence on $CaCO_3$ production rates using multiple linear regression analysis with an adjusted coefficient of determination, using

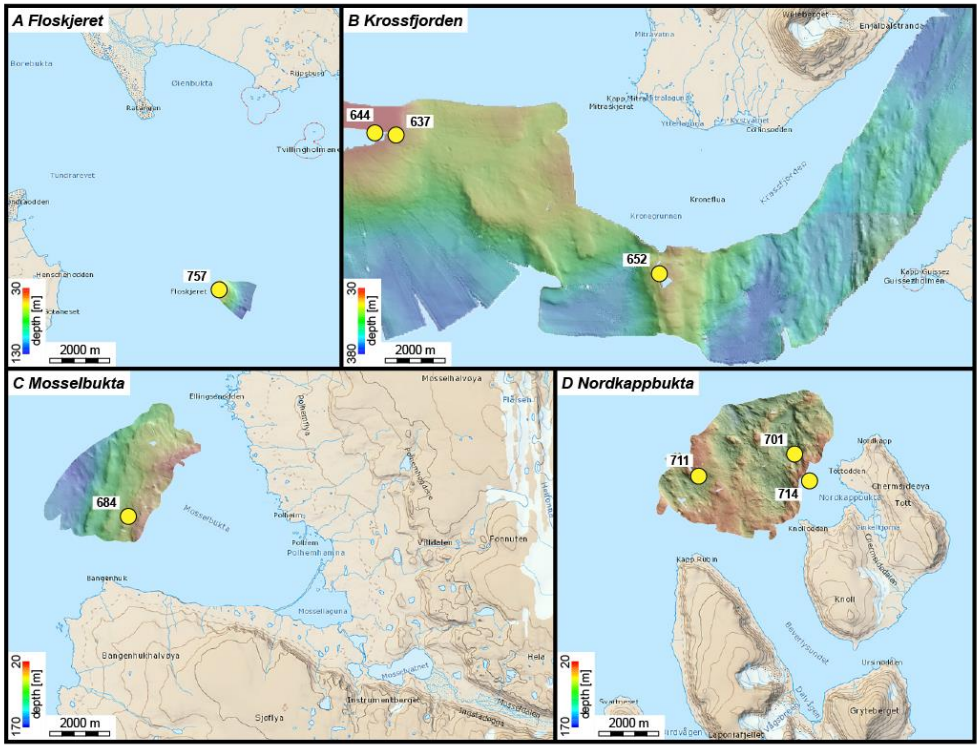

Fig. 2. The sampling sites in order from south to north being Floskjeret in Isfjorden **(A)**, Krossfjorden at the eastern coast of Haakon VII Land **(B)**, Mosselbukta at the eastern coast of Mosselhalvøya **(C)**, and Nordkappbukta at the northern coast of Nordaustlandet **(D)**; yellow dots indicate the coralline red algal and rhodolith sampling sites; note the different water depth scales; topographic map extracts are used with courtesy of the Norwegian Polar Institute.

the equation

$$R^2_{\text{adj}} = 1 - \frac{(1-R^2)(n-1)}{n-k-1},$$

with n being the number of points and k being the number of independent variables. All calculations were carried out using the palaeontological statistics software package PAST (Hammer et al., 2001).

3 Results

3.1 Seafloor and rhodolith bed properties

The seafloor at each site mainly consists of moraine gravels (probably Late Weichselian; Ottesen et al., 2007) and dropstones. In this glaciogenic environment, the rhodolith and coralline red algal communities appear as a dominating feature. The properties of these communities slightly vary along the different dive tracks, but show the same overall pattern. Initial growth of coralline red algae starts at ca. 78 m water depth and, with further shallowing, the development of the coralline red algae continuously increases (i.e. the protuberances are bigger and grow denser) and the first rhodoliths appear. With further shallowing, the coverage with coralline

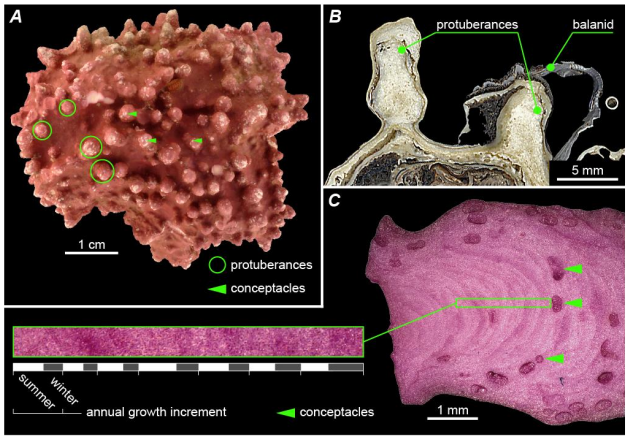

Fig. 3. Monospecific rhodolith consisting of *Lithothamnion glaciale* Kjellman, 1883, with distinct protuberances (green circles) and visible conceptacles (green arrows) that contain the spores **(A)**, the protuberances are the main spots of $CaCO_3$ production in the coralline red algal tissue **(B)**, presumably annual growth increments divided in bright, heavily calcified summer bands and dark, less calcified winter bands, the width of the annual forming conceptacles (green arrows) corresponds to the increment pattern **(C)**.

Table 2. Sampling sites (FK = Floskjeret, KF = Krossfjorden, MB = Mosselbukta, NKB = Nordkappbukta) from south to north together with the number of rhodoliths used for analysis. Protuberance counting together with digital image analysis led to the median number of protuberances per square metre rhodolith surface. Annual growth increment counting led to the mean $CaCO_3$ production per protuberance per year, calculated from the number of the annual growth increments in relation to protuberance weight. Levene's test shows levels of significance.

			Protuberances/surface [n m^{-2}]				Weight/annual growth increment [mg n^{-2}]			
Locality code	Site #	Samples [n]	Median	Min	Max	Levene's test	Median	Min	Max	Levene's test
FK	757	17	35 239	14 454	55 636	$p = 0.0079$	5.86	3.00	11.18	$p < 0.0001$
KF	652	2	55 302	51 248	55 302	$p < 0.0001$	3.07	2.25	3.93	$p = 0.0011$
KF	637	31	71 096	30 446	141 810	$p < 0.0001$	2.55	1.43	4.21	$p < 0.0001$
KF	644	15	59 673	22 903	105 201	$p = 0.0102$	2.84	1.82	4.24	$p < 0.0001$
MB	684	27	28 499	19 380	60 094	$p = 0.0003$	4.20	2.17	8.41	$p < 0.0001$
NKB	714	37	30 740	9953	65 088	$p = 0.0001$	5.13	2.59	9.64	$p < 0.0001$
NKB	711	28	21 404	8946	46 883	$p = 0.0011$	4.92	2.54	8.32	$p < 0.0001$
NKB	701	10	22 179	11 967	40 903	$p = 0.1214$	4.55	1.55	8.57	$p < 0.0001$

red algae and rhodoliths strongly increases up to 100 % (with varying percentages of coralline red algae and rhodoliths).

The coralline red algal and rhodolith communities of Floskjeret and Nordkappbukta are composed of *Lithothamnion glaciale* Kjellman, 1883, and *Phymatolithon tenue* (Rosenvinge) Düwel and Wegeberg, 1996, while *L. glaciale* is always the dominating alga. The coralline algal rhodolith communities of Krossfjorden and Mosselbukta are composed of *L. glaciale* only. At Floskjeret, Krossfjorden, and Mosselbukta, *L. glaciale* grows as unattached rhodoliths and also attached to cobbles. At Nordkappbukta, *L. glaciale* additionally grows attached to bedrock. Rhodoliths are more or less spherical to ovoidal to more irregular in form, consist largely of knobby protuberances (branches), and are nucleated or hollow. Attached thalli produce short (up to 19 mm) warty or knobby protuberances of varying diameter from a crustose base. Thalli of *P. tenue* grow attached to cobbles or, in the case of Nordkappbukta, even to bedrock, and occur intermixed with *L. glaciale*.

3.2 $CaCO_3$ production rates

The median numbers of protuberances per square metre at each site calculated from protuberance counting on the digitally measured rhodolith surfaces are compiled in Table 2.

Age estimation using increment counting together with the determined weight of each protuberance led to the annual mean production of $CaCO_3$ per protuberance. The annual weight increase is linear (Fig. 4; Table 2), so variably old protuberances can be used for calculation purposes.

The combination of both values, protuberances per square metre and $CaCO_3$ production per protuberance per year, led to the annual $CaCO_3$ production rate of each rhodolith community in g ($CaCO_3$) m^{-2} yr^{-1} (Table 3). Plotting these values against the possibly influencing parameters showed that correlations for water depth are not significant (Fig. 5a). A significant correlation is visible for seawater calcite saturation, but contrary to what one would expect (Fig. 5b). Significant correlations are evident for the annual mean temperature, the geographical latitude, the duration of the polar night, and the duration of sea ice cover (Fig. 5c–f). Multiple linear regression analysis showed that geographical latitude and duration of the polar night are the main controls, followed by the duration of sea ice cover, while the annual mean temperature is less influential (Table 4).

4 Discussion

As stated before, a comparison of the Svalbard $CaCO_3$ production rates with data from other surveys is not reasonable due to different taxa from various water depths, analysed by various methods. On these grounds, our study yields an opportunity to show the influence of different parameters on rhodolith $CaCO_3$ production rates from different populations.

The four sites are well comparable with regard to their Arctic environment, influenced by the warm West Spitsbergen Current, the cold East Spitsbergen Current, sea ice formation, annual meltwater discharge, and a strong seasonality of the light levels (Harland, 1997; Svendsen et al., 2002; Sapota et al., 2009). Teichert et al. (2012, 2014) also showed obvious similarities between the populations, with *Lithothamnion glaciale* as the dominating photoautotrophic organism at water depths around 45 m, appearing as encrustations or rhodoliths. The colonized substrate is mainly made up of glaciogenic debris and dropstones, and grazing organisms like chitons and echinoids are present at all sites, presumably contributing to keep the rhodoliths free from epibionts (Steneck, 1986). The rhodoliths also act as bioengineers sensu Jones et al. (1994) and provide microenvironments for the benthic organisms, which therefore depend on substantial rhodolith growth.

Table 3. Annual $CaCO_3$ production rates per square metre per year at each site (FK = Floskjeret, KF = Krossfjorden, MB = Mosselbukta, NKB = Nordkappbukta), calculated from the mean weight per annual growth increment and the median number of protuberances per rhodolith surface, together with the possibly influencing parameters, being depth [m] = water depth in metres; lat. [°N] = geographical latitude in decimal degrees; polar night [d] = duration of the polar night in days, data from USNO Sun Rise Tables (2013); sea ice [mo] = mean duration of sea ice cover in months, data from Svendsen et al. (2002); Nilsen et al. (2008); Spreen et al. (2008); AMSR-E Sea Ice Maps (2013); AMT [°C] = annual mean temperature in degrees Celsius, data from LEVITUS 94 (2013); Ω_{Cal} = calcite saturation of the seawater, data (snapshot conditions) from Teichert et al. (2012, 2014); note increased $CaCO_3$ production rate in combination with deviating water depth at NKB #714.

Locality code	Site #	Annual $CaCO_3$ production [g m^{-2} yr^{-1}]	Depth [m]	Lat. [° N]	Polar night [d]	Sea ice [mo]	AMT [°C]	Ω_{Cal}
FK	757	200.3	45	78.3113	113	4	1.5	1.44
KF	652	169.8	47	79.0618	117	6	0.7	2.67
KF	637	181.5	50	79.0985	118	6	0.7	1.45
KF	644	181.5	41	79.0986	118	6	0.7	1.45
MB	684	119.8	44	79.8946	122	7	0.7	2.59
NKB	714	157.7	27	80.5251	126	10	0.5	2.86
NKB	711	105.3	45	80.5293	126	10	0.5	2.86
NKB	701	100.9	38	80.5335	126	10	0.5	2.86

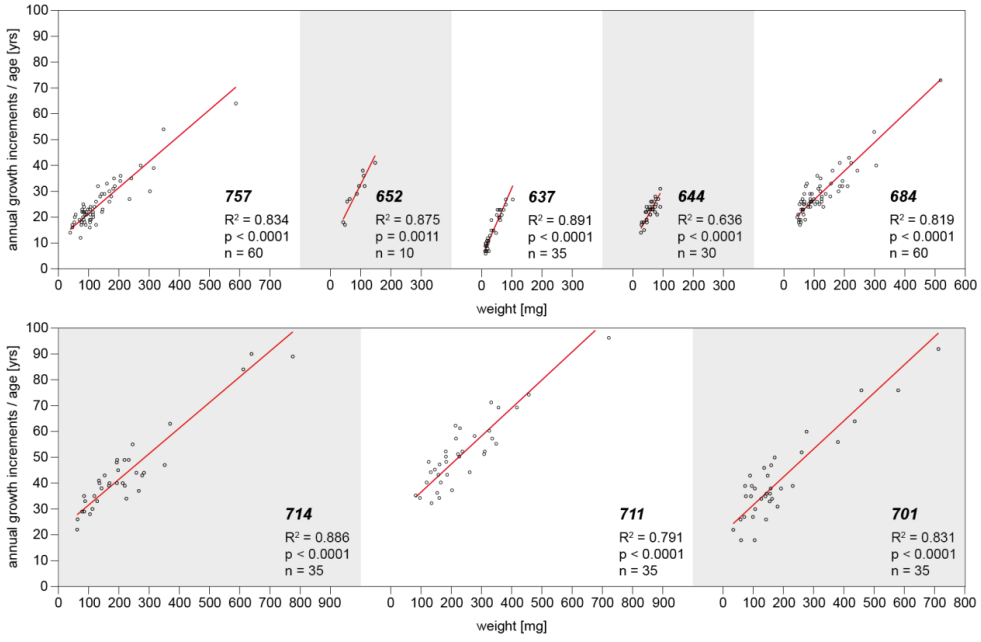

Fig. 4. Scatter plots indicating the linear $CaCO_3$ accretion within the protuberances using reduced major axis algorithm and Levene's test for homogeneity of variance based on means (one-way ANOVA).

To gain data on the annual rhodolith $CaCO_3$ production, a method was used that enabled the analysis of large sample sizes. This analysis is based on the assumptions that (1) the growth increments counted in the protuberances of *L. glaciale* are annual and that (2) the increase in weight with age is linear, so specimens of different ages can be compared. Assumption (2) is confirmed by the findings shown in Fig. 4, indicating a significantly linear weight increase with age, but there has been discussion on the nature of coralline red algal banding patterns, ranging from daily over lunar to annual cycles (Bosence, 1980; Freiwald and Henrich, 1994). The coralline red algal calcification process involves high magnesium calcite precipitation within most cell walls (Kamenos et al., 2009). Early electron microscope work showed that the calcified cell walls of coralline algae have a two-layered structure, an inner layer of acicular calcite parallel to the cell wall, succeeded by radial, inward growing calcite crystals (Alexandersson, 1977; Garbary, 1978; Cabioch and Giraud, 1986). Because the underlying biomineralization process takes place only during the growth period (Bosence, 1991), the result is a growth pattern starting with heavily calcified cell rows at the beginning of the growth period and grading

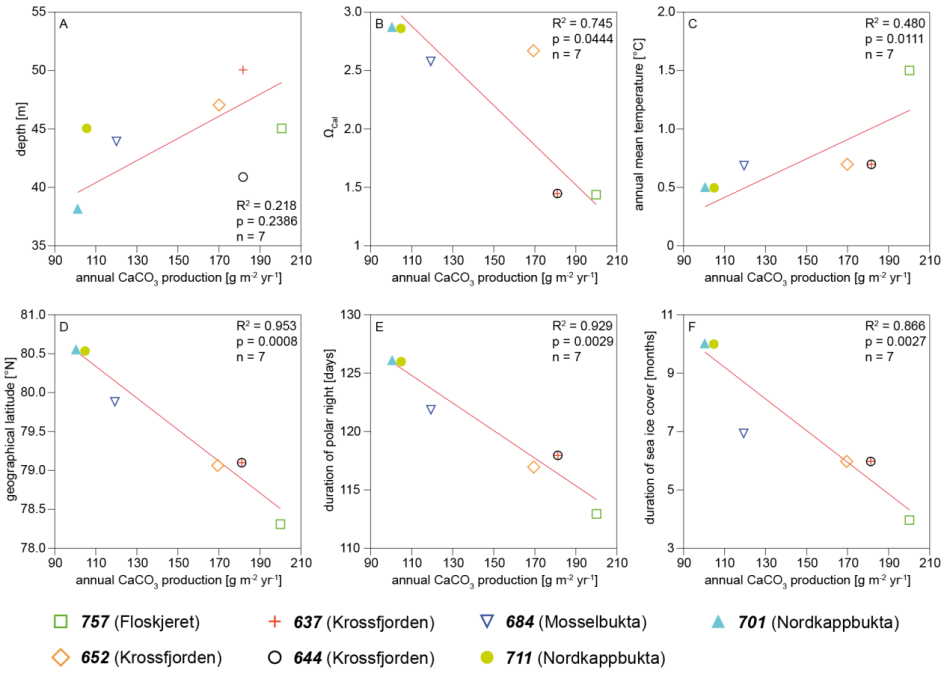

Fig. 5. Correlations between the annual $CaCO_3$ production rates [g $(CaCO_3)$ m^{-2} yr^{-1}] and physical parameters using reduced major axis algorithm and Levene's test for homogeneity of variance based on means (one-way ANOVA), showing no significance for water depth **(A)**, "inverse" significance for calcite saturation of the seawater **(B)**, and significance for the annual mean temperature **(C)**, the geographical latitude **(D)**, the duration of the polar night **(E)**, and the duration of sea ice cover **(F)**.

Table 4. Multiple linear regression analysis showing the relative influence of geographical latitude, duration of the polar night, duration of sea ice cover, and annual mean temperature (independent variables) on the annual $CaCO_3$ production rate (dependent variable).

Multiple $R^2_{adj} = 0.99935$		
ANOVA		
$F = 763.78$ $p = 0.0013$		
Variable	p	R^2
Annual $CaCO_3$ production rate	$= 0.0053$	
Geographical latitude	$= 0.0070$	0.95302
Duration of the polar night	$= 0.0220$	0.92871
Duration of sea ice cover	$= 0.0657$	0.86575
Annual mean temperature	$= 0.0301$	0.4802

into less calcified cell rows towards the end of the growth period (see also Fig. 3c). In our experiments, the visibility of that pattern has been amplified using fuchsine staining, resulting in bright, heavily calcified summer bands (i.e. there is little cell lumen/pore cavity to bind the fuchsine staining) and dark, less calcified winter bands (i.e. there is more cell lumen/pore cavity to bind the fuchsine staining).

The assumption of an annual banding pattern is hardened by the distribution of the reproductive conceptacles in the protuberances of *L. glaciale*. These conceptacles contain the spores of the plants, form annually (Jackson, 2003), and clearly parallel the longitudinal, fuchsine-stained growth increments in the protuberance sections (Fig. 3c). Due to their spatial distribution in the protuberances, conceptacles are not visible on the cut face at all increments, but their thickness corresponds to the growth increments.

For those reasons, we assume an annual banding pattern exhibited by our specimens. On the other hand, we appreciate that the nature of the growth pattern still has to be proven by growth experiments under laboratory conditions. However, because we applied the same presuppositions for all sites, comparability of the potentially controlling factors is given.

The calculated $CaCO_3$ production rates (Table 3) significantly differ between the sites, suggesting that they are influenced by physical parameters, since the coralline red algae all belong to the same species and share similar biotic communities in terms of the associated organisms. The other constant for all sites is water depth, except for station 714 in 27 m water depth, with a relatively high $CaCO_3$ production due to increased irradiance levels. Because of that, site 714 was excluded from the coherence plots in Fig. 5. For the remaining sites, the following parameters were considered: geographical latitude, mean duration of sea ice cover, duration of the polar night, annual mean temperature, water depth, and calcite saturation of the water column (Table 3). Annual meltwater discharge has no impact on the coralline

red algal communities, which prevail in at least 38 m water depth, while meltwater does not fully intermix with the water body and only affects the uppermost ~ 20 m of the water column (Teichert et al., 2012, 2014).

Geographical latitude, mean duration of sea ice cover, and duration of the polar night are directly linked to irradiance, the obviously most important feature influencing coralline red algal growth (Kain and Norton, 1990), and show significant correlations (Fig. 5d–f). Due to earth's axis obliquity, the duration of the polar night prolongs with increasing geographical latitude, leading to a shortened growth period towards higher latitudes. Additionally, the angle of solar radiation flattens with increasing geographical latitude, leading to decreased radiation intensity. This is directly reflected in the $CaCO_3$ production rates, because biomineralization takes place only during the growth period (Bosence, 1991), also resulting in the incremental banding pattern, starting with heavily calcified cell rows at the beginning of the growth period and grading into less calcified cell rows towards the end of the growth period (see also Fig. 3c). The same applies for the mean duration of the sea ice cover, which reduces the light transmitted through the water column to a minimum. Despite the high correlation in our data, this has to be considered conservative, because the AMSR-E Sea Ice database only provides information for the last 10 yr, while the oldest examined protuberances expose maximum ages of > 90 yr (Fig. 4, stations 711, 701). Nevertheless, the influence of geographical parameters linked to irradiance on the rhodolith $CaCO_3$ production rates is significant, and multiple linear regression analysis (Table 4) shows that these are the most important controls. The reason why the importance of the geographical latitude slightly superimposes the duration of the polar night is that this duration is a function of geographical latitude, which additionally holds the feature of a flattened angle of light incidence.

Another correlating parameter is the annual mean temperature (Fig. 5c). Regarding coralline red algae, the optimum temperature varies geographically and with species, but the general pattern shows an increase in growth rate to a maximum that is near the top of the tolerated range (Kain and Norton, 1990). This is directly reflected in our calculations, with $CaCO_3$ production rates decreasing linearly with the annual mean temperature, so rising temperatures as a response to global warming could apparently lead to an increased algal growth rate.

By contrast, water depth does not seem to influence the $CaCO_3$ production rates (Fig. 5a), which is easy to explain, because all depths are nearly the same, ranging in the dysphotic zone (Teichert et al., 2012, 2014), so it is superimposed by the effects above.

$CaCO_3$ production rates (Fig. 5b) appear to increase with decreasing calcite saturation, which is unexpected because coralline red algae are heavily calcifying organisms. Nevertheless, coralline red algae may induce a microenvironment suitable for $CaCO_3$ precipitation by metabolic excretion of alginic acid (Alexandersson, 1977; Okazaki et al., 1982), so the degree of carbonate saturation could be of minor importance as long as $\Omega_{Cal} \geq 1$. Another possibility might be that the concomitant grazers are more affected by less saturated seawater, and the coralline red algae are less affected by abrasion, although no information is available. Though, in case of calcite undersaturation ($\Omega_{Cal} < 1$), the impact would be significant as Martin et al. (2008) showed experimentally for acidified seawater that led to a strong reduction in coralline red algal cover. With respect to the ongoing climate change, one can say that it will have distinctive impacts on the rhodolith communities.

There will be no change in the angle of light incidence and the duration of the polar night, because these are subject to astronomic parameters. A development that already can be observed is the reduced sea ice formation due to increased temperatures (Shapiro et al., 2003). On the one hand, this may result in a prolonged growth period and, together with risen temperatures, would favour the coralline red algae, but it is more likely that climate warming will lead to global runoff increase (Labat et al., 2004). This would confront the coralline red algae with an increased amount of fine sediments in the water column and consequently light transmission decrease. Additionally, it has been shown experimentally that smothering of coralline red algae with fine sediments is likely to lead to a dieback of the algal thalli (Wilson et al., 2004). Since multiple regression analysis (Table 4) shows that the geographical parameters linked to irradiance are most influential on coralline red algae while temperature is rather subordinated, the positive effects of increased temperatures on the $CaCO_3$ production rates will most likely be outranged by the decreased light incidence.

5 Conclusions

Our study shows that light is the most important physical parameter influencing the rhodolith communities at Svalbard, followed by the annual mean temperature. While the angle of solar incidence and the duration of the polar night will not be subject to global change, increased weathering due to rising temperatures will likely result in reduced rhodolith $CaCO_3$ production rates. Because the rhodoliths act as bioengineering organisms and are inhabited by a variety of benthic taxa, changes will expand on the whole prevailing ecosystem.

Acknowledgements. This work was funded by the Deutsche Forschungsgemeinschaft (FR 1134/18). The authors would like to thank the captain and the crew of Maria S. Merian, the JAGO operating team (GEOMAR), and Ines Pyko for her work as research assistant.

Edited by: S. Pantoja

References

Adey, W. H.: The genus *Phymatolithon* in the Gulf of Maine, Hydrobiologia, 24, 377–420, 1964.

Adey, W. H.: Distribution of saxicolous crustose corallines in the northwestern North Atlantic, J. Phycol., 2, 49–54, 1966.

Adey, W. H.: The effects of light and temperature on growth rates in boreal-subarctic crustose corallines, J. Phycol., 6, 269–276, 1970.

Adey, W. H. and McKibbin, D. L.: Studies on the maerl species *Phymatolithon calcareum* (Pallas) nov. comb. and *Lithothamnion corallioides* Crouan in the Ria de Vigo, Bot. Mar., 13, 100–106, 1970.

Adey, W. H., Chamberlain, Y. M., and Irvine, L. M.: An SEM-based analysis of the morphology, anatomy, and reproduction of *Lithothamnion tophiforme* (Esper) Unger (Corallinales, Rhodophyta), with a comparative study of associated North Atlantic arctic/subarctic Melobesioideae, J. Phycol., 41, 1010–1024, 2005.

Agegian, C. R., Mackenzie, F. T., Tribble, J. S., and Sabine, C.: Carbonate production and flux from a mid-depth bank ecosystem, Penguin Bank, Hawaii, in: Biogeochemical cycling and fluxes between the deep euphotic zone and other oceanic realms, edited by: Agegian, C. R., National Undersea Research Program, 88, 5–32, 1988.

Alexandersson, E. T.: Carbonate cementation in recent coralline algal constructions, in: Fossil algae: Recent results and developments, edited by: Flügel, E., Springer, Berlin, 261–269, 1977.

AMSR-E Sea Ice Maps: database comprising the AMSR-E sea ice concentrations calculated daily in near real time, part of the GMES project Polar View and of the Arctic Regional Ocean Observing System (Arctic ROOS), available at: http://www.iup.uni-bremen.de:8084/amsr/, last access: March 2013.

Arias, C., Masse, J.-P., and Vilas, L.: Hauterivian shallow marine calcareous biogenic mounds: S.E. Spain, Palaeogeogr. Palaeocl., 119, 3–17, 1995.

Basso, D.: Carbonate production by calcareous red algae and global change, Geodiversitas, 34, 13–33, 2012.

Bosence, D.: Sedimentary facies, production rates and facies models for recent coralline algal gravels, Co. Galway, Ireland, Geol. J., 15, 91–111, 1980.

Bosence, D. W. J.: Description and classification of Rhodoliths (Rhodoids, Rhodolites), in: Coated grains, edited by: Peryt, T. M., Springer, Berlin, Heidelberg, 217–224, 1983.

Bosence, D. W. J.: Coralline algae: mineralization, taxonomy, and palaeoecology, in: Calcareous algae and stromatolites, edited by: Riding, R., Springer, Heidelberg, 98–113, 1991.

Bosence, D. and Wilson, J.: Maerl growth, carbonate production rates and accumulation rates in the northeast Atlantic, Aquat. Conserv., 13, 21–31, 2003.

Bucur, I. I., Kiessling, W., and Scasso, R. A.: Re-description and neotypification of *Archamphiroa jurassica* Steinmann 1930, a calcareous red alga from the Jurassic of Argentina, J. Paleontol., 83, 962–986, 2009.

Cabioch, J. and Giraud, G.: Structural aspects of biomineralization in the coralline algae (calcified Rhodophyceae), in: Biomineralization in lower plants and animals, edited by: Leadbetter, B. S. C. and Riding, R., University Press, Oxford, 141–156, 1986.

Canals, M. and Ballesteros, E.: Production of carbonates particles by phytobenthic communities on the Mallorca-Menorca shelf, northwestern Mediterranean Sea, Deep-Sea Res.-Pt. II, 44, 611–629, 1997.

Chisholm, J. R. M.: Calcification by crustose coralline algae on the northern Great Barrier Reef, Australia, Limnol. Oceanogr., 45, 1476–1484, 2000.

Edyvean, R. G. J. and Ford, H.: Growth rates of *Lithophyllum incrustans* (Corallinales, Rhodophyta) from South West Wales, Brit. Phycol. J., 22, 139–146, 1987.

El Haïkali, B. E., Bensoussan, N., Romano, J. C., and Bousquet, V.: Estimation of photosynthesis and calcification rates of *Corallina elongata* Ellis and Solander, 1786, by measurements of dissolved oxygen, pH and total alkalinity, Sci. Mar., 86, 45–56, 2004.

Foster, M. S.: Rhodoliths: between rocks and soft places, J. Phycol., 37, 659–667, 2001.

Foster, M. S., Mcconnico, L. M., Lundsten, L., Wadsworth, T., Kimball, T., Brooks, L. B., Medina-López, M., Riosmena-Rodríguez, R., Hernández-Carmona, G., Vásquez-Elizondo, R. M., Johnson, S., and Steller, D. L.: Diversity and natural history of a *Lithothamnion muelleri–Sargassum horridum* community in the Gulf of California, Cienc. Mar., 33, 367–384, 2007.

Frantz, B. R., Kashgarian, M., Coale, K. H., and Foster, M. S.: Growth rate and potential climate record from a rhodolith using ^{14}C accelerator mass spectrometry, Limnol. Oceanogr., 45, 1773–1777, 2000.

Freiwald, A. and Henrich, R.: Reefal coralline algal build-ups within the Arctic Circle: Morphology and sedimentary dynamics under extreme environmental seasonality, Sedimentology, 41, 963–984, 1994.

Garbary, D. J.: An introduction to the scanning electron microscopy of the red algae, Syst. Ass. Spec. Pub., 10, 205–222, 1978.

Gherardi, D. F. M.: Community structure and carbonate production of a temperate rhodolith bank from Arvoredo Island, southern Brazil, Braz. J. Oceanogr., 52, 207–224, 2004.

Halfar, J., Zack, T., Kronz, A., and Zachos, J. C.: Growth and high-resolution paleoenvironmental signals of rhodoliths (coralline red algae): A new biogenic archive, J. Geophys. Res., 105, 107–122, 2000.

Halfar, J., Williams, B., Hetzinger, S., Steneck, R., Lebednik, P. A., Winsborough, C., Omar, A., Chan, P., and Wanamaker Jr., A. D.: 225 years of Bering Sea climate and ecosystem dynamics revealed by coralline algal growth-increment widths, Geology, 39, 579–582, 2011.

Hammer, Ø., Harper, D. A. T., and Ryan, P. D.: PAST: Paleontological statistics software package for education and data analysis, Palaeontol. Electron., 4, 9 pp., 2001.

Harland, W. B.: The geology of Svalbard, Geological Society Memoirs, The Geological Society, London, 1997.

Irvine, L. M. and Chamberlain, Y. M.: Seaweeds of the British Isles, Rhodophyta Part 2B Corallinales, Hildenbrandiales, London, The Natural History Museum, London, 1994.

Jackson, A.: *Lithothamnion glaciale*. Maerl. Marine Life Information Network: Biology and Sensitivity Key Information Sub-programme, Plymouth: Marine Biological Association of the United Kingdom, available at: http://www.marlin.ac.uk/reproduction.php?speciesID=3711 (last access: November 2012), 2003.

Jones, C. G., Lawton, J. H., and Shachak, M.: Organisms as ecosystem engineers, Oikos, 69, 373–386, 1994.

Kain, J. M. and Norton, T. A.: Marine ecology, in: Biology of the red algae, edited by: Cole, K. M. and Sheath, R. G., Cambridge University Press, 1990.

Kamenos, N. A., Cusack, M., and Moore, P. G.: Coralline algae are global palaeothermometers with bi-weekly resolution, Geochim. Cosmochim. Ac., 72, 771–779, 2008.

Kamenos, N. A., Cusack, M., Huthwelker, T., Lagarde, P., and Scheibling, R. E.: Mg-lattice associations in red coralline algae, Geochim. Cosmochim. Ac., 73, 1901–1907, 2009.

Kjellman, F. R.: Norra Ishafvets Algflora, Vega-expeditionens Vetenskapliga Iaktagelser, 3, 1–431, 1883 (in Swedish).

Kjellman, F. R.: The algae of the Arctic Sea, Kongliga Svenska Vetenskaps-Akademien Handligar, 20, 1–350, 1885.

Labat, D., Goddéris, Y., Probst, J. L., and Guyot, J. L.: Evidence for global runoff increase related to climate warming, Adv. Water Resour., 27, 631–642, 2004.

LEVITUS 94: database comprising the World Ocean Atlas 1994 (WOA94), an atlas of objectively analyzed fields of major ocean parameters at the annual, seasonal, and monthly time scales, available at: http://iridl.ldeo.columbia.edu/SOURCES/.LEVITUS94/, last access: March 2013.

Lherminier, P., Meincke, J., Freiwald, A., and Schauer, U.: Circulation and Ecosystems in the Subpolar and Polar North Atlantic, Universität Hamburg, Hamburg, 174, 2009.

Martin, S., Castets, M.-D., and Clavier, J.: Primary production, respiration and calcification of the temperate free-living coralline alga Lithothamnion corallioides, Aquat. Bot., 85, 121–128, 2006.

Martin, S., Rodolfo-Metalpa, R., Ransome, E., Rowley, S., Buia, M.-C., Gattuso, J.-P., and Hall-Spencer, J.: Effects of naturally acidified seawater on seagrass calcareous epibionts, Biol. Lett., 4, 689–692, 2008.

Maytone, P. T.: Quantifying growth and calcium carbonate deposition of *Calliarthron cheilosporioides* (Corallinales, Rhodophyta) in the field using a persistent vital stain, J. Phycol., 46, 13–17, 2010.

Nilsen, F., Cottier, F., Skogseth, R., and Mattsson, S.: Fjord-shelf exchanges controlled by ice and brine production: The interannual variation of Atlantic Waters in Isfjorden, Svalbard, Cont. Shelf Res., 28, 1838–1853, 2008.

Okazaki, M., Furunga, K., Tsukayama, K., and Nisizawa, K.: Isolation and identification of alginic acid from a calcareous red alga *Serraticardia maxima*, Bot. Mar., 25, 123–131, 1982.

Ottesen, D., Dowdeswell, J. A., Landvik, J. Y., and Mienert, J.: Dynamics of the Late Weichselian ice sheet on Svalbard inferred from high-resolution sea-floor morphology, Boreas, 36, 286–306, 2007.

Payri, C. E.: *Hydrolithon reinboldii* rhodolith distribution, growth and carbon production of a French Polynesian reef, in: Proceedings of the Eighth International Coral Reef Symposium (Panama City 1996), edited by: Lessios, H. A. and Macintyre, I. G., Smithsonian Tropical Research Institute, Balboa, Panama, 755–760, 1997.

Potin, P., Floc'h, J. Y., Augris, C., and Cabioch, J.: Annual growth rate of the calcareous red alga *Lithothamnion corallioides* (Corallinales, Rhodophyta) in the Bay of Brest, France, Hydrobiologia, 204–205, 263–267, 1990.

Sapota, G., Wojtasik, B., Burska, D., and Nowiński, K.: Persistent organic pollutants (POPs) and polycyclic aromatic hydrocarbons (PAHs) in surface sediments from selected fjords, tidal plains and lakes of the north Spitsbergen, Pol. Polar Res., 30, 59–76, 2009.

Savini, A., Basso, D., Bracchi, V. A., Corselli, C., and Pennetta, M.: Maerl-bed mapping and carbonate quantification on submerged terraces offshore the Cilento peninsula (Tyrrhenian Sea, Italy), in: Calcareous algae and global change: From identification to quantification, edited by: Basso, D. and Granier, B., Geodiversitas, 34, 77–98, 2012.

Schäfer, P., Fortunato, H., Bader, B., Liebetrau, V., Bauch, T., and Reijmer, J. J. G.: Growth rates and carbonate production by coralline red algae in upwelling and non-upwelling settings along the Pacific coast of Panama, Palaios, 26, 420–432, 2011.

Schlagintweit, F.: *Iberpora bodeuri* Granier & Berthou 2002 (*incertae sedis*) from the Plassen Formation (Kimmeridgian-Berriasian) of the Tethyan Realm, Geol. Croat., 57, 1–13, 2004.

Shapiro, I., Colony, R., and Vinje, T.: April sea ice extent in the Barents Sea, 1850–2001, Polar Res., 22, 5–10, 2003.

Spreen, G., Kaleschke, L., and Heygster, G.: Sea ice remote sensing using AMSR-E 89-GHz channels: J. Geophys. Res., 113, C02S03, doi:10.1029/2005JC003384, 2008.

Stearn, C. W., Scoffin, T. P., and Martindale, W.: Calcium Carbonate Budget of a fringing reef on the west coast of Barbados. I. Zonation and Productivity, B. Mar. Sci., 27, 479–510, 1977.

Steller, D. L., Hernández-Ayón, J. M., Riosmena-Rodriguez, R., and Cabello-Pasini, A.: Effects of temperature on photosynthesis, growth and calcification rates of the free-living coralline alga *Lithophyllum margaritae*, Cienc. Mar., 33, 441–456, 2007.

Steneck, R. S.: The ecology of coralline algal crusts: Convergent patterns and adaptive strategies, Annu. Rev. Ecol. Syst., 17, 273–303, 1986.

Svendsen, H., Beszczynska-Møller, A., Hagen, J. O., Lefauconnier, B., Tverberg, V., Gerland, S., Ørbæk, J. B., Bischof, K., Papucci, C., Zajaczkowski, M., Azzolini, R., Bruland, O., Wiencke, C., Winther, J. G., and Dallmann, W.: The physical environment of Kongsfjorden-Krossfjorden, an Arctic fjord system in Svalbard, Polar Res., 21, 133–166, 2002.

Teichert, S., Woelkerling, W. J., Rüggeberg, A., Wisshak, M., Piepenburg, D., Meyerhöfer, M., Form, A., and Freiwald, A.: Rhodolith beds (Corallinales, Rhodophyta) and their physical and biological environment at 80°31′ N in Nordkappbukta (Nordaustlandet, Svalbard Archipelago, Norway), Phycologia, 51, 371–390, 2012.

Teichert, S., Woelkerling, W. J., Rüggeberg, A., Wisshak, M., Piepenburg, D., Meyerhöfer, M., Form, A., and Freiwald, A.: Arctic rhodolith beds and their environmental controls, Facies, 60, 15–37, doi:10.1007/s10347-013-0372-2, 2014.

USNO Sun Rise Tables: database comprising the United States Naval Observatory (USNO) providing astronomical data, available at: http://aa.usno.navy.mil/data/docs/RS_OneYear.php, last access: March 2013.

Walker, D. and Woelkerling, W. J.: Quantitative study of sediment contribution by epiphytic coralline red algae in seagrass meadows in Shark Bay, Western Australia, Mar. Ecol.-Prog. Ser., 43, 71–77, 1988.

Wilson, S., Blake, C., Berges, J. A., and Maggs, C. A.: Environmental tolerances of free-living coralline algae (maerl): Implications for European marine conservation, Biol. Conserv., 120, 279–289, 2004.